Neuron, Volume *89*

Supplemental Information

A Systems-Level Analysis of the Peripheral Nerve Intrinsic Axonal Growth Program

Vijayendran Chandran, Giovanni Coppola, Homaira Nawabi, Takao Omura, Revital Versano, Eric A. Huebner, Alice Zhang, Michael Costigan, Ajay Yekkirala, Lee Barrett, Armin Blesch, Izhak Michaelevski, Jeremy Davis-Turak, Fuying Gao, Peter Langfelder, Steve Horvath, Zhigang He, Larry Benowitz, Mike Fainzilber, Mark Tuszynski, Clifford J. Woolf, and Daniel H. Geschwind

Figure S1

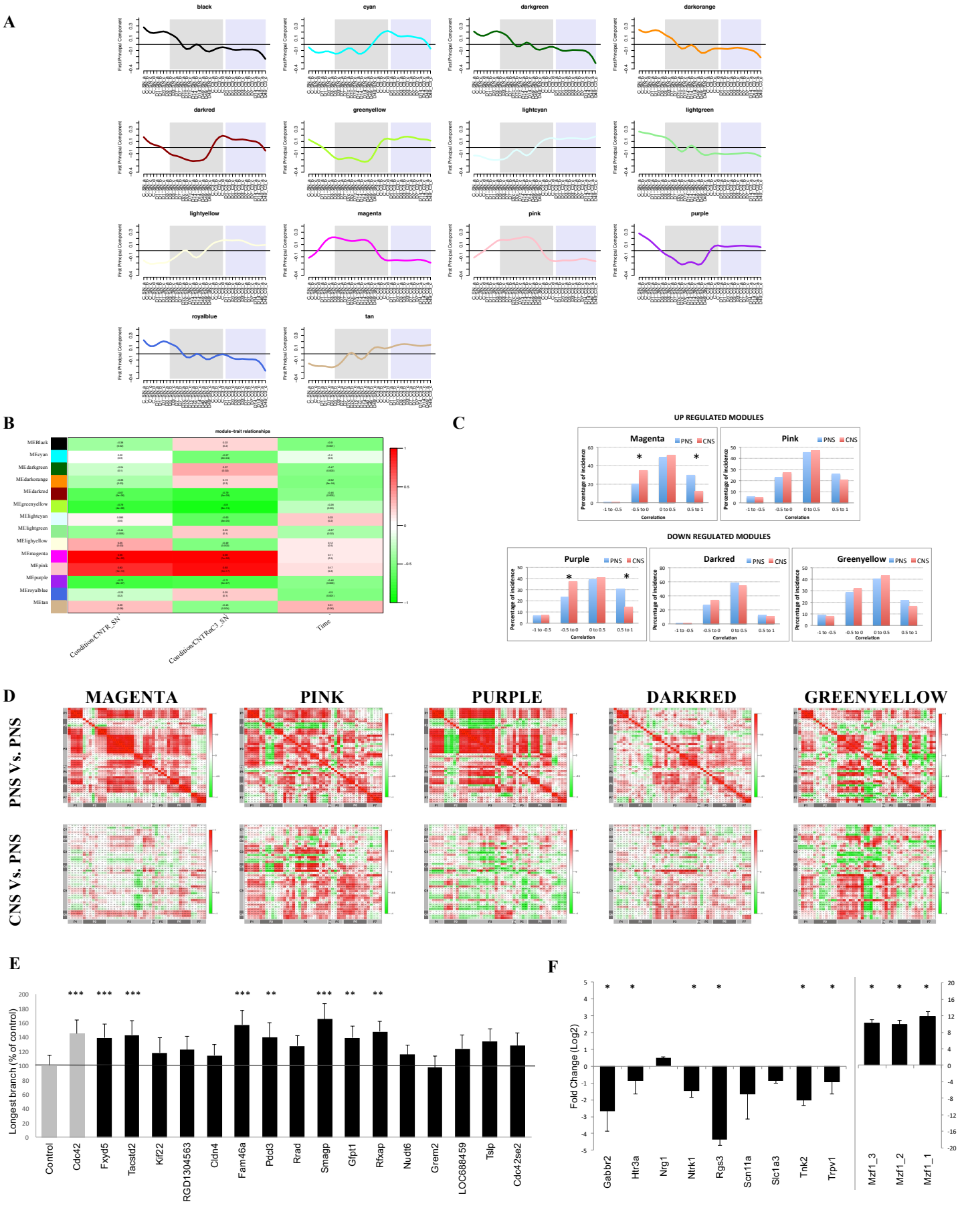
A
black
cyan
darkgreen
darkorange
darkred
greenyellow
lightcyan
lightgreen
lightyellow
magenta
pink
purple
royalblue
tan
First Principal Component
B
module−trait relationships
MEBlack
MEcyan
MEdarkgreen
MEdarkorange
MEdarkred
MEgreenyellow
MElightcyan
MElightgreen
MElightyellow
MEmagenta
MEpink
MEpurple
MEroyalblue
MEtan
Condition:CNTR_SN
Condition:CNTRdC3_SN
Time
C
UP REGULATED MODULES
Magenta
Pink
DOWN REGULATED MODULES
Purple
Darkred
Greenyellow
PNS
CNS
Percentage of incidence
Correlation
-1 to -0.5
-0.5 to 0
0 to 0.5
0.5 to 1
D
MAGENTA
PINK
PURPLE
DARKRED
GREENYELLOW
PNS Vs. PNS
CNS Vs. PNS
E
Longest branch (% of control)
Control
Cdc42
Fxyd5
Tacstd2
Kif22
RGD1304563
Cldn4
Fam46a
Pdcl3
Rrad
Smagp
Gfpt1
Rtkap
Nudt6
Grem2
LOC688459
Tslp
Cdc42se2
F
Fold Change (Log2)
Gabbr2
Htr3a
Nrg1
Ntrk1
Rgs3
Scn11a
Slc1a3
Tnk2
Trpv1
Mzf1_3
Mzf1_2
Mzf1_1

Figure S2


PNS Injury
CNS Injury
SN Lesion (Days)
0_Day 1_Day 3_Day 7_Day 14_Day 49_Day
Mild Spinal Cord Injury
0.5_Hour 4_Hour 1_Day 7_day 14_day
SN Lesion (Hours)
0_Hour 1_Hour 3_Hour 8_Hour 12_Hour 18_Hour 24_Hour 28_Hour
Moderate Spinal Cord Injury
4_Hour 1_Day 2_Day 3_Day 7_day
Spinal Nerve Ligation
0_Day 3_Day 7_Day 21_Day 40_Day
Severe Spinal Cord Injury
4_Hour 1_day 7_day 14_day
Chronic Nerve Constriction
0_Day 3_Day 7_Day 21_Day 40_Day
Complete Spinal Cord Injury
0_Day 2_Day 7_Day 21_Day 60_Day
Spared Nerve Injury
0_Day 3_Day 7_Day 21_Day 40_Day
Moderate Spinal Cord Injury
4_Hours 24_Hour 7_Day 14_Day 28_Day 3_Month
ATF2 ATF5 BATF BCL6 BHLHE40 CRX EGR1 EGR2 ERG ETS1 FLI1
FOS FOSL1 FOSL2 HSF1 JUN JUNB JUND KLF1 KLF4 KLF5 MYC
MZF1 NFKB1 NFYA NR2C2 PPARA RELA REST SMAD1 SP1 SP2 SP3
SP4 SRF STAT1 STAT3 STAT4 STAT5A STAT5B TCF3 TCFCP2L1 TP53 ZFX

Figure S3

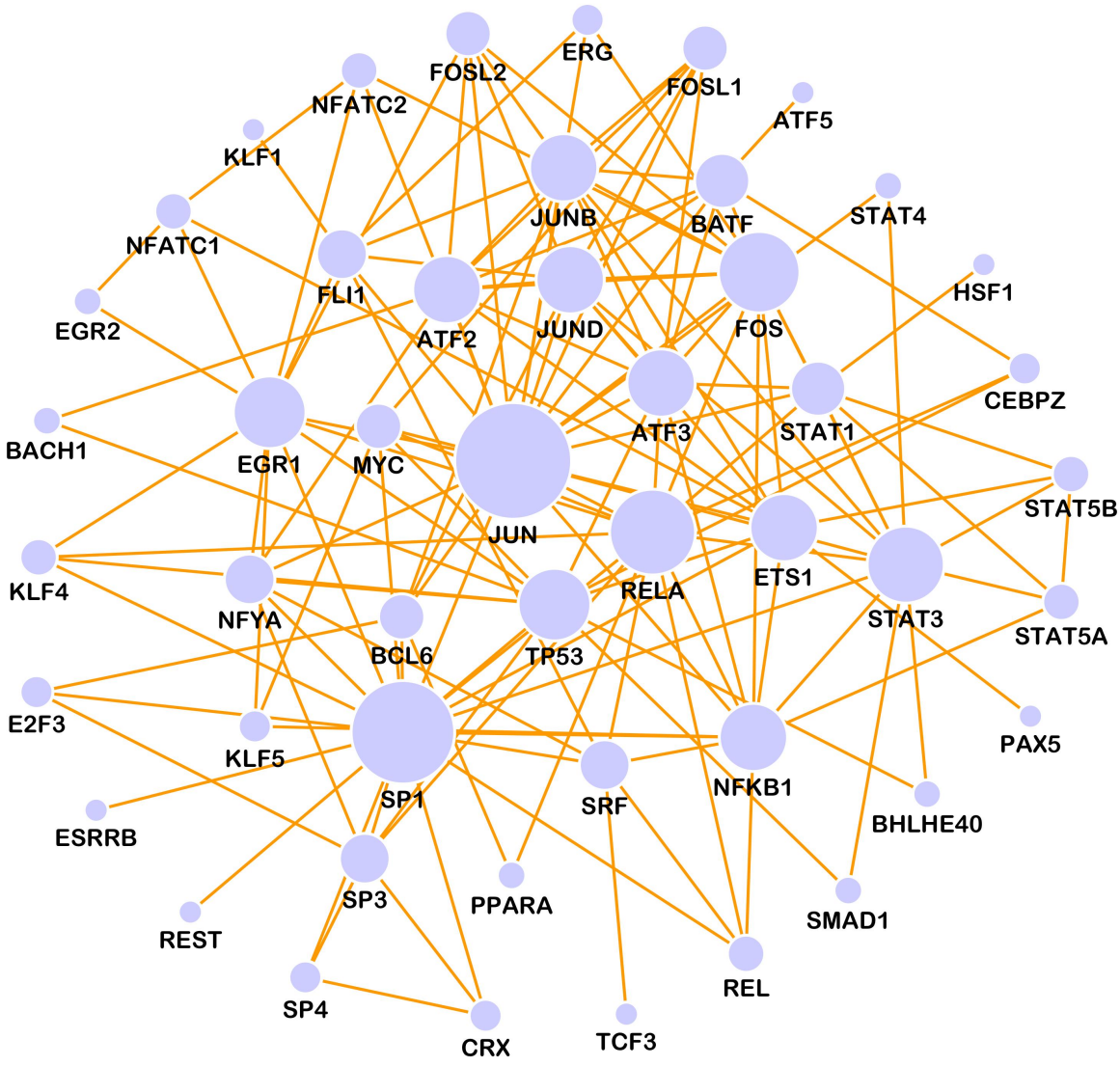
FOSL2
ERG
FOSL1
NFATC2
ATF5
KLF1
JUNB
BATF
STAT4
NFATC1
FLI1
HSF1
EGR2
ATF2
JUND
FOS
CEBPZ
ATF3
STAT1
BACH1
EGR1
MYC
STAT5B
JUN
KLF4
ETS1
RELA
NFYA
STAT3
STAT5A
BCL6
TP53
E2F3
PAX5
KLF5
NFKB1
SP1
SRF
ESRRB
BHLHE40
SP3
PPARA
SMAD1
REST
REL
SP4
CRX
TCF3

Figure S4

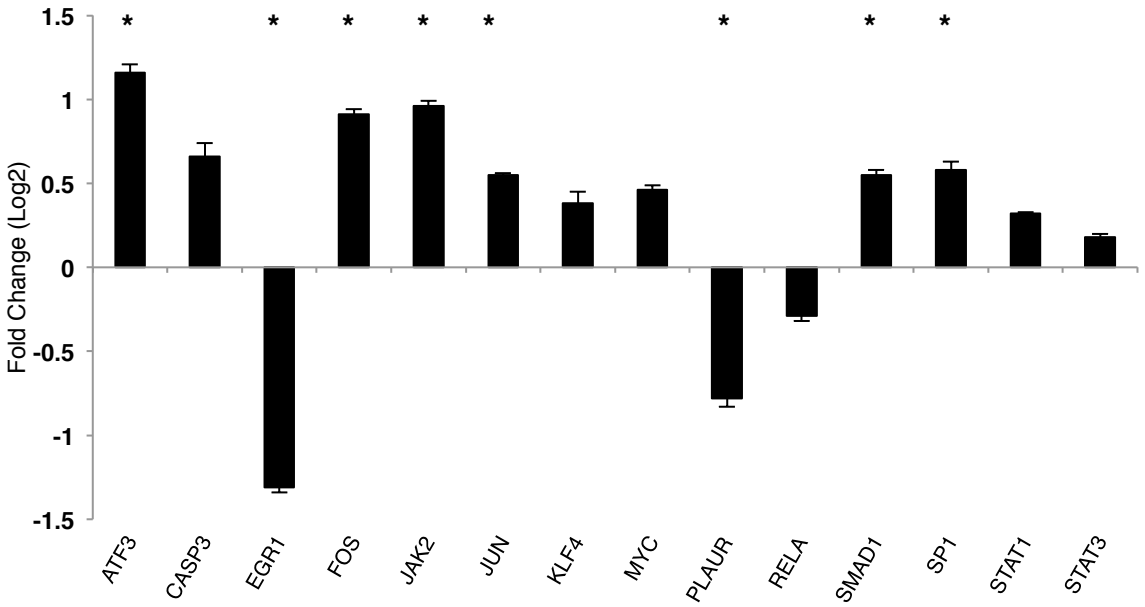
1.5
1
0.5
0
-0.5
-1
-1.5
Fold Change (Log2)
*
*
*
*
*
*
*
ATF3
CASP3
EGR1
FOS
JAK2
JUN
KLF4
MYC
PLAUR
RELA
SMAD1
SP1
STAT1
STAT3

Figure S5

A

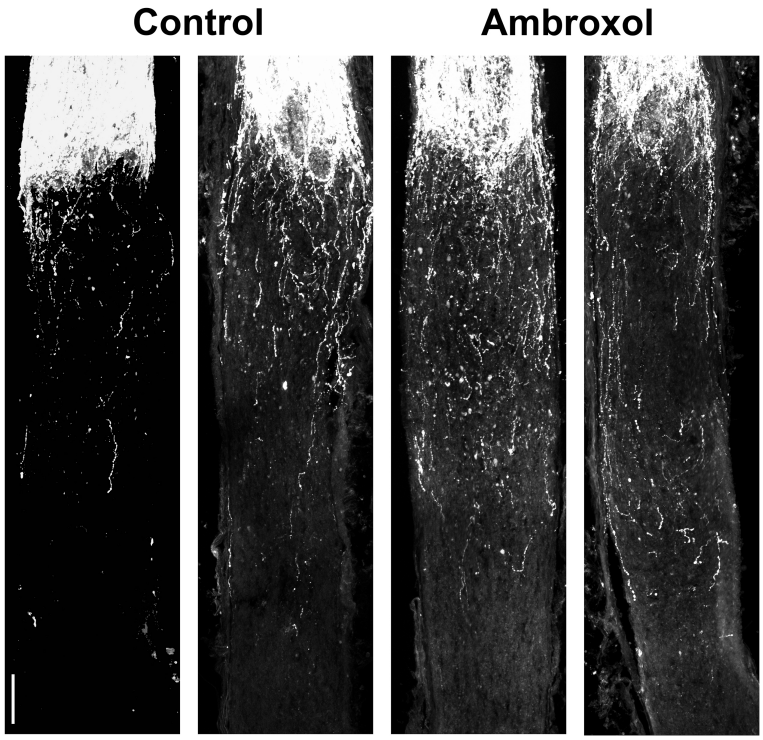
Control
Ambroxol

B

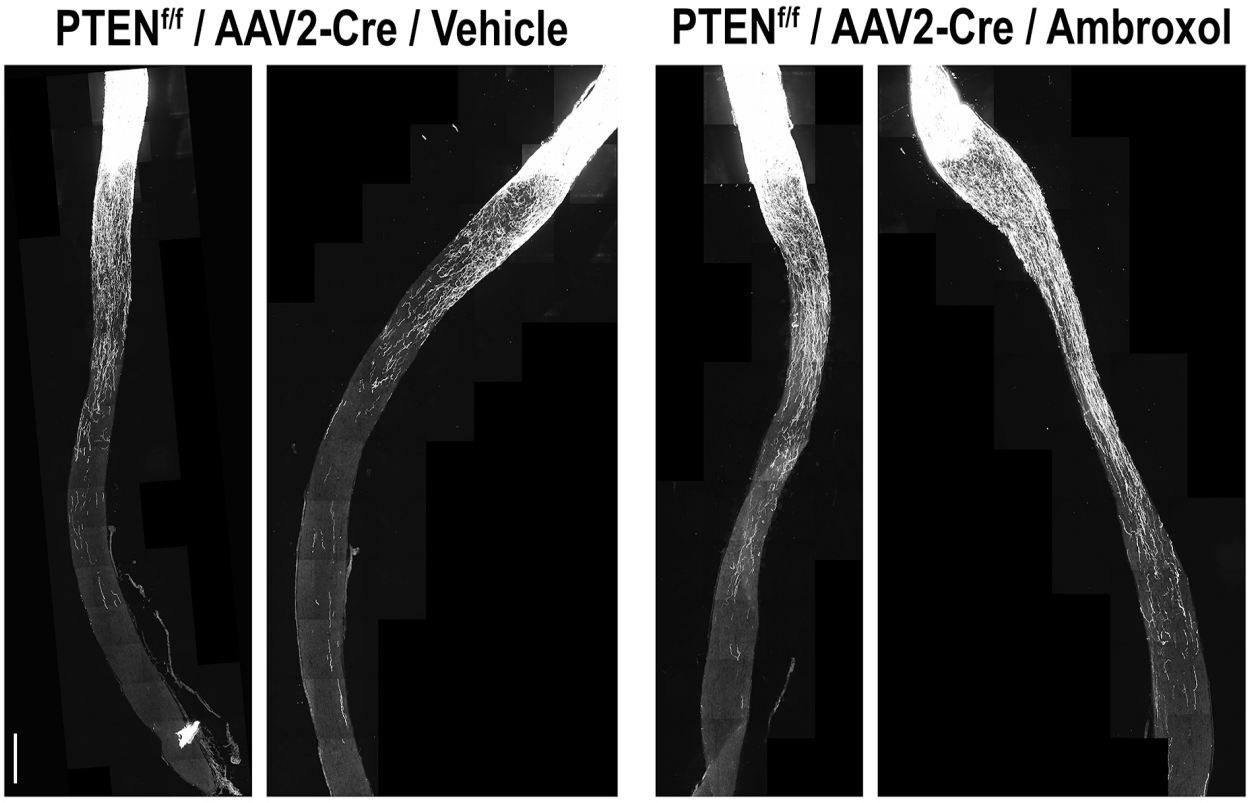
PTEN$^{f/f}$ / AAV2-Cre / Vehicle
PTEN$^{f/f}$ / AAV2-Cre / Ambroxol

Supplemental Figure Legends:

Figure S1. Consensus Modules After Sciatic Nerve Injury, Related to Figure 1 and 3. (A) Fourteen consensus modules shared between the two SN lesion datasets showing module eigengene correlation with time-dependent changes after injury. Within the plot, white and gray corresponds to the SN lesion dataset and blue corresponds to the C3 lesion dataset generated at 1, 3, 7, 14 and 49 days after injury (samples are arranged from left to right in an ascending order – days 1-49). (B) Correlations between coexpression module eigengenes and the nerve injury process. In each cell, the Pearson correlation coefficient is shown with the corresponding p-value in brackets below. Cells in the table are color coded using correlation values according to color scale on the right, that is high positive correlations are denoted by deeper red color, and high negative correlations by deeper green color. (C) Histogram of correlation values comparing the direction of correlation based on the gene expression levels of the top 50 hub genes in each identified modules in 16 (8 PNS and 8 CNS) independent datasets related to PNS and CNS neuronal injury. Lower triangular correlation matrix generated from pairwise PNS versus PNS and PNS versus CNS datasets were utilized to generate these histogram plots. (D) For each identified modules, the calculated matrix whose elements are the pairwise correlation scores between each datasets analyzed (PNS Vs. PNS datasets and PNS Vs. CNS datasets) is visualized as a colored map. The correlation scores are encoded with a color gradient from − 1 (green, completely anti-correlated) to + 1 (red, completely correlated). (E) Differences in the longest neurite branch by over-expression of 16 cDNA clones in DRG neurons with *Cdc42*, as a positive control. Longest neurite per neuron was quantified using Neuromath software, from 50-150 cells per view. Significant differences determined by ANOVA with a Bonferroni-Holm post hoc test. (F) Differential mRNA expression for candidate MZF1 target genes in downregulated modules by qPCR of DRG neurons overexpressing MZF1 (5 days) is shown. T-test * $p < 0.05$.

Figure S2. Over-Represented TFs are Differentially Expressed During PNS and CNS Injury, Related to Figure 3 and 4. Time series gene expression profiles (relative mRNA expression level – log2) of over-represented TFs from 10 independent datasets (see Table S1, S4) after CNS or PNS injury are shown. Microarray data sets are available from the Gene Expression Omnibus (see Table S4). PNS and CNS dataset were obtained, read into R, and preprocessed using the "expresso" function and the MAS5 method of preprocessing, which benchmarked four commonly used normalization procedures (MAS5, RMA, GCRMA and LiWong) (see Experimental Procedures). We then calculated the correlation of gene expression between samples, and outliers with mean sample correlations more than two to three standard deviations below average were omitted until no outliers remained (Oldham et al., 2008). Finally, quantile normalization was performed on the filtered data to examine differential expression. We analyzed these normalized microarray data sets generated from different laboratories after PNS and CNS lesion to generate time series expression plots of the candidate transcription factors. The expression levels of highly expressed transcription factor *Atf3* is not shown in these plots for clarity purposes. Over-represented TFs are co-expressed and significantly up-regulated after PNS injury in multiple data sets, where as in the CNS injury datasets the levels of these TFs were significantly variable or down-regulated (see also Figure 4E).

Figure S3. Protein–Protein Interaction Network of the Over-Represented TFs, Related to Figure 4. Candidate transcription factors were screened for all possible combinations of protein pairs having experimentally verified human interaction data in the STRING database (string-db.org). Each node represents proteins, node size are based on their degree and the edges represent experimentally validated protein-protein interaction (see Experimental Procedures).

Figure S4. Quantitative Real-Time RT-PCR after Treatment of Candidate Drug, Related to Figure 5. Differential expression of mRNA for critical genes in PPI network validated by qPCR of DRG neurons treated with Ambroxol. DRG neurons were treated with 60mM ambroxol for 4 days and the expression levels of the hub genes selected from the PPI network (Figure 6A) were measured by q-RT-PCR, using *Gapdh* as internal control. T-test * $p < 0.05$.

Figure S5. Ambroxol promotes retinal ganglion cell axonal regeneration. Related to Figure 5 and 6. (A) Representative confocal images of optic nerve sections from WT (C57BL/6) animal treated with vehicle (n=10) and WT (C57BL/6) animal treated with ambroxol (25mg/ml, n=13). Measurements shown in Figure 5 and 6 were made blinded to treatment. (B) Representative confocal images of optic nerve sections from $PTEN^{-/-}$ animal (infected with AAV2-Cre) treated with vehicle ($PTEN^{f/f}$ / AAV2-Cre / Vehicle) and $PTEN^{-/-}$ animal (infected with AAV2-Cre) treated with ambroxol ($PTEN^{f/f}$ / AAV2-Cre / Ambroxol). Axons are labeled with CTB. Scale bar: 100μm.

Table S1

Dataset No	Lab	No. of Arrays	Experiment	Time	Reference
1	Mark Tuszynski	16	DRG (L4,5,6) after SN lesion (vs. naïve)	0, 3, 7, 14 Days	(Blesch et al., 2012)
2	Mark Tuszynski	25	DRG after C3 lesion (vs. naïve)	0, 3, 7, 14 Days	(Kadoya et al., 2009)
3	Mike Fainzilber	43	DRG after SN lesion (vs. sham)	1, 3, 8, 12, 16, 18, 24, 28 hrs	(Michaelevski et al., 2010)
4	Clifford Woolf	21	DRG after spinal nerve ligation (vs. sham)	0, 3, 7, 21, 40 Days	(Costigan et al., 2002)
5	Clifford Woolf	21	DRG after spared nerve injury (vs. sham)	0, 3, 7, 21, 40 Days	(Costigan et al., 2002)
6	Clifford Woolf	21	DRG after chronic nerve constriction (vs. sham)	0, 3, 7, 21, 40 Days	(Costigan et al., 2002)
	Arrays:	147	Time points:	31	

Table S3

Module	GO annotation clusters	No of GO terms	No of Genes
Magenta (530)	Cluster 1: Regulation of transcription related	16	70
Up-regulated	Cluster 2: Stimulus related	12	56
	Cluster 3: Inflammation/wounding related	7	48
	Cluster 4: Apoptosis related	9	38
	Cluster 5: Signaling related	2	29
	Cluster 6: Cell proliferation/growth related	4	25
	Cluster 7: Neuron differentiation	1	22
	Cluster 8: Cell migration related	5	13
Pink (131)	Cluster 1: Extracellular matrix/region related	7	22
Up-regulated			
Purple (281)	Cluster 1: Plasma membrane related	2	55
Down-regulated	Cluster 2: Ion/gated channel activity related	17	32
	Cluster 3: Ion binding related	2	26
	Cluster 4: Synapse/cell junction related	4	17
Darkred (57)	Cluster 1: Ion binding related	2	18
Down-regulated	Cluster 2: Ion/gated channel activity related	10	15
Greenyellow (112)	Not Significant	NA	NA
Down-regulated			

Table S4.

Dataset No	No. of Arrays	Experiment Type	Experiment	GEO Id	Reference (PMID)
P1	16 samples (12 injured)	Peripheral nerve injury	DRG (L4,5,6) after Sciatic nerve lesion during 0, 3, 7, 14 days	N/A	(Blesch et al., 2012)
P2	72 samples (21 sham, 51 injured)	Peripheral nerve injury	Sciatic nerve lesion. Adult rat L4 and L5 DRGs cells after 1,3,8,12,16,18,24, and 28 hours after a sciatic nerve (proximal and distal) lesion.	GEO: GSE26350	(Michaelevski et al., 2010)
P3.1	44 samples (21 sham, 23 injured)	Peripheral nerve injury	Spinal Nerve Ligation and Spared Nerve Injury. Adult rat L4 and L5 DRGs cells after 3,7,21,40 hours.	GEO: GSE30691	(Costigan et al., 2010; Ma et al., 2011)
P3.2	12 samples (12 injured)	Peripheral nerve injury	Chronic Constriction Injury. Adult rat L4 and L5 DRGs cells after 3,7,21,40 hours.	GEO: GSE30691	(Costigan et al., 2010; Ma et al., 2011)
P4	10 samples (5 control, 5 injured)	Peripheral nerve injury	DRG after Spinal Nerve Lesion (vs. sham)	N/A	(Costigan et al., 2002)
P5	36 samples (12 sham, 24 inured)	Peripheral nerve injury	DRGs from L4 and L5 spinal nerve ligation model of neuropathic pain in the rat (at 28 and 50 days)	GEO: GSE2884	N/A
P6	24 samples (24 injured)	Peripheral nerve injury	Sciatic nerve crush at 12, 24, 72 hours and 7 days. Lumbar DRGs L4, L5 and L6.	GEO: GSE21007	(Geeven et al., 2011)
P7	18 samples (0 to 9 hours injured)	Peripheral nerve injury	Proximal sciatic nerve (SN) tissues (0.5cm) at 0h, 0.5h, 1h, 3h, 6h and 9h after sciatic nerve resection.	GEO: GSE33175	(Wang et al., 2012)
C1	15 samples (15 injured)	Motor cortex injury	Gene expression analysis of motor cortex after spinal C3 lesion.	GEO: GSE76679	N/A
C2	5 samples (5 injured)	Optic nerve injury	Retinal ganglion cells (RGCs) after 4 d post lens injury –with lens injury	N/A	(Fischer et al., 2004)
C3	5 samples (5 injured)	Optic nerve injury	Retinal ganglion cells (RGCs) after 4 d post lens injury –without lens injury	N/A	(Fischer et al., 2004)
C4	5 samples (5 control)	Optic nerve injury (control)	Retinal ganglion cells (RGCs) after 4 d post lens injury	N/A	(Fischer et al., 2004)
C5.1	41 (19 control, 22 mild)	Spinal cord injury	Mild spinal cord injury at thoracic vertebrae T9 at various time points up to 28 days post injury.	GEO: GDS63	(Di Giovanni et al., 2003)
C5.2	29 (29 moderate)	Spinal cord injury	Moderate spinal cord injury at thoracic vertebrae T9 at various time points up to 28 days post injury.	GEO: GDS63	(Di Giovanni et al., 2003)
C5.3	19 (19 severe)	Spinal cord injury	Severe spinal cord injury at thoracic vertebrae T9 at various time points up to 28 days post injury.	GEO: GDS63	(Di Giovanni et al., 2003)
C6	31 samples (31 injured)	Spinal cord transection	Gene expression changes were studied in rat tail motor neurones 0, 2, 7, 21 and 60 days after comlete spinal transection.	GEO: GSE19701	(Ryge et al., 2010)
	Total Arrays: 382				

Table S7.

GENE NAME	PRIMER NAME	SEQ
AKT1	AKT1_L1	CCACGCTACTTCCTCCTCAA
	AKT1_R1	CAGCGGATGATGAAGGTGTT
ATF3	ATF3_MR_L	CCAGGTCTCTGCCTCAGAAG
	ATF3_MR_R	CATCTCCAGGGGTCTGTTGT
CASP3	CASP3_RM_F	AAGATCACAGCAAAAGGAGCA
	CASP3_RM_R	GAGTTTCGGCTTTCCAGTCA
CDC42	CDC42_L1	TTGATACTGCAGGGCAAGAG
	CDC42_R1	TGAGTTATCTCAGGCACCCA
EGR1	EGR1_RM_F	ATTTTTCCTGAGCCCCAAAG
	EGR1_RM_R	CTGGGTACGGTTCTCCAGAC
FOS	FOS_MR_L	CCATGATGTTCTCGGGTTTC
	FOS_MR_R	TGTCACCGTGGGGATAAAGT
FXYD5	FXYD5_2_L1	TCCCAGATCCAGATCAAACC
	FXYD5_2_R1	GGGTACCTTTCTTGCTGCTT
GABBR2	GABBR2_RM_F	TGTTTGGCAGCAAGTACCAG
	GABBR2_RM_R	GCTGTGGAGTCTTCCCTGAG
GAP43	GAP43_2_L1	CAGGAAAGATCCCAAGTCCA
	GAP43_2_R1	GAACGGAACATTGCACACAC
GFPT1	GFPT1_L1	TTGTGTCCCTCGTGATGTTT
	GFPT1_R1	CCTTAATCAAGTCCGGCAGT
HTR3A	HTR3A_RM_F	CATGTATGCCATCCTCAACG
	HTR3A_RM_R	CCACGTCCACAAACTCATTG
JAK2	JAK2_RM_F	GAAGCAGCAAGCATGATGAG
	JAK2_RM_R	GGCCACTCCAAGTTTCCATA
JUN	JUN_L1	ACATGCTCAGGGAACAGGTG
	JUN_R1	TCAAAACGTTTGCAACTGCTG
KLF4	KLF4_RM_F	GTGCCCCAAGATTAAGCAAG
	KLF4_RM_R	GTGACAGTCCCTGCTGTTCA
MAPK1	MAPK1_L1	TGCGCTTCAGACATGAGAAC
	MAPK1_R1	TCTGTCTCCATGAGGTCCTGT
MYC	MYC_RM_F	GAGGGCCAAGTTGGACAGT
	MYC_RM_R	GCCTTTTCGTTGTTTTCCAA
MZF1	MZF1_1M_F	CTCTGGTGAAGCTGGAGGAC
	MZF1_1M_R	GCACCTGTTCCTTGGAATGT
MZF1	MZF1_2M_F	AAGATCCACACAGGCGAGAG
	MZF1_2M_R	AAGCTCTGGCCACACTCTGT
MZF1	MZF1_3M_F	TCTAATCTCACCCAGCACCA
	MZF1_3M_R	TAGGGCTTCTCGCCAGTATG
NRG1	NRG1_RM_F	CAAAAGAACCAAGCCCAATG
	NRG1_RM_R	TGCTGGGTTAGTCCTGCTCT
NTRK1	NTRK1_RM_F	GTCTGGTGGGTCAGGGACTA
	NTRK1_RM_R	GGTGAAGATCTCCCAGAGCA
PLAUR	PLAUR_RM_F	CACAGCAGGTTTCCATAGCA
	PLAUR_RM_R	CCCAGCACATCTAAGCCTGT
RELA	RELA_RM_F	ATTAGCCAGCGAATCCAGAC
	RELA_RM_R	ATCTTGAGCTCGGCAGTGTT
RGS3	RGS3_RM_F	CTGTTTGCCTACTCGGACCT
	RGS3_RM_R	CTTCTTCTGCTCCTGCGAGT
SCN11A	SCN11A_RM_F	ATTCTGGGGCCTTTTAATCC
	SCN11A_RM_R	CAATGAAGCCTCTTGCCAAT
SLC1A3	SLC1A3_RM_F	GCCATTTTCATCGCTCAAGT
	SLC1A3_RM_R	CAGAAACCAGTCCACTGCAA

SMAD1	SMAD1_RM_F	AGGCACAGCGAGTACAATCC
	SMAD1_RM_R	GAGTGAGGGTAGGTGCTGCT
SMAGP	SMAGP_L1	GCGCTCATTGCAGTTGTTAT
	SMAGP_R1	TCTGCAGGCTCATAGGTGAC
SP1	SP1_RM_F	AAGCCCAGACAATCACCTTG
	SP1_RM_R	GCACCTGGATCCCTGAAGTA
STAT1	STAT1_RM_F	CCCCATGGAAATCAGACAGT
	STAT1_RM_R	TCCTGGAGATTACGCTTGCT
STAT3	STAT3_L1	GGAGCAGAGATGTGGGAATG
	STAT3_R1	TGGCAAGGAGTGGGTCTCTA
TACSTD2	TACSTD2_2_L1	CACCGCTGCTACTGCTACTG
	TACSTD2_2_R1	GCAGGCACTTGGAAGTTAGC
TNK2	TNK2_RM_F	GCCTGAAGACACGGACTTTC
	TNK2_RM_R	CAGCACTGGACCATGACATT
TRPV1	TRPV1_RM_F	GCTAACGGGGACTTCTTCAA
	TRPV1_RM_R	TGTGTTATCTGCCACCTCCA

Supplemental Table Legends:

Table S1. Datasets, Related to Figure 1 and Experimental Procedures. Time series datasets used for initial computational meta-analysis, which were obtained from various nerve injury models and different laboratories.

Table S2. (A) Gene List Associated with Consensus Modules after Sciatic Nerve Injury, Related to Figure 1. Fourteen consensus modules shared between the two SN lesion datasets are denoted along with genes in these modules. The connectivity and ranking scores are provided. **(B) Literature Annotation of Genes in Regeneration Associated Module.** Table providing the magenta module's association with neuronal regeneration based on the published literature by testing association with the key-words neuronal regeneration, axonal regeneration, and nerve injury in the PubMed database for every gene. The total number of hits and publications for each gene are represented.

Table S3. Gene Ontology Analysis of Nerve Injury Associated Modules, Related to Figure 1. For categorization and clustering of GO terms, we considered GO terms with Benjamini-corrected P-values less than 0.05. The total number of genes present in each module is represented within brackets.

Table S4. PNS and CNS Nerve Injury Related Datasets used for Validation, Related to Figure 1 and S1. Table summarizing sixteen nerve injury related datasets independent from those used in the initial analysis used for validation analyses. Sixteen (8 PNS and 8 CNS) datasets related to PNS and CNS neuronal injury consisting of 382 microarrays was studied to examine the consistency of the co-expression networks. Microarray data sets were downloaded from the Gene Expression Omnibus.

Table S5. Analysis of Transcription-Factor Binding-Sites (TFBS) Enrichment, Related to Figure 3. For estimation of TFBSs enrichment in the identified corresponding module-genelist (genes having ≥ 0.5 average connectivity) promoter sequences (1000bp upstream from transcription start site), P-values were obtained relative to three background datasets: 1000-bp of sequence upstream of all rat gene, rat CpG islands and rat chromosome 20 (see Experimental Procedures). Enriched TFBS position weight matrices from both JASPAR and TRANSFAC databases are provided in this table. Literature associations for each TF are also provided with PubMed association/co-occurrence of corresponding TF with the tags - neuronal regeneration, axonal regeneration, nerve injury.

Table S6. (A) Integration of ChIP data to identify potential targets of enriched transcription factors, Related to Figure 3. To identify TF targets, we screened the existing ChIP data for TFs from either ENCODE (Landt et al., 2012) or other compiled genome-wide ChIP data (Lachmann et al., 2010) to generate a regulatory network (Fig. 2A). Enriched TFs, their corresponding targets and their associated gene co-expression modules are provided. **(B) Analysis of Transcription-Factor Binding-Sites (TFBS) Enrichment in Rat, Mouse and Humans.** TFBS enrichment analysis was performed for corresponding module-genelist promoter sequences obtained from rat, and their orthologous genes obtained from mouse and humans. For estimation of TFBSs enrichment in the corresponding module-genelist, we screened the promoter sequences (1000bp upstream from transcription start site) for enrichment by obtaining P-values relative to three background datasets: 1000-bp sequences upstream of all rat gene, rat CpG islands and rat chromosome 20 (see Experimental Procedures).

Table S7. Primer Pairs, Related to Figures 3 and S4. Table with primer-template pairs used in this study.

Extended Experimental Procedures:

Data Set Acquisition and Filtering

Microarray data sets were downloaded from the Gene Expression Omnibus (GEO), read into R, and preprocessed using the "expresso" function and the MAS5 method of preprocessing, which benchmarked four commonly used normalization procedures (MAS5, RMA, GCRMA and LiWong) (Lim et al., 2007). We then calculated the correlation of gene expression between samples, and outliers with mean sample correlations more than two to three standard deviations below average were omitted until no outliers remained. Finally, quantile normalization was performed on the filtered data to examine differential expression. We analyzed three different microarray data sets generated from two different laboratories after SN (sciatic nerve) and C3 lesion to generate the initial regeneration-associated co-expression network (see below). We used additional three different data sets for validating these co-expression networks. In total this included - 6 datasets, 147 arrays and 31 time points (see Table S1). We analyzed another separate group of 16 datasets (382 arrays) related to neuronal injury (8 PNS and 8 CNS) to examine the consistency of the co-expression networks (see Table S4).

Construction of RAG Co-expression Networks

A weighted gene co-expression network was constructed for each dataset to identify groups of genes (modules) associated with temporal pattern of expression changes after nerve injury following a previously described algorithm (Oldham et al., 2006; Zhang and Horvath, 2005). Briefly, we first computed the Pearson correlation between each pair of selected genes yielding a similarity (correlation) matrix. Next, the adjacency matrix was calculated by raising the absolute values of the correlation matrix to a power (β) as described previously (Zhang and Horvath, 2005). The parameter β was chosen by using the scale-free topology criterion (Zhang and Horvath, 2005), such that the resulting network connectivity distribution best approximated scale-free topology. The adjacency matrix was then used to define a measure of node dissimilarity, based on the topological overlap matrix, a biologically meaningful measure of node similarity (Zhang and Horvath, 2005). Next, the probe sets were hierarchically clustered using the distance measure and modules were determined by choosing a height cutoff for the resulting dendrogram by using a dynamic tree-cutting algorithm (Zhang and Horvath, 2005).

Consensus Module Analyses, Module and Gene Selection

Consensus modules are defined as sets of highly connected nodes that can be found in multiple networks generated from different nerve injury datasets. Consensus modules were identified using a suitable consensus dissimilarity that were used as input to a clustering procedure, analogous to the procedure for identifying modules in individual sets as described elsewhere (Langfelder and Horvath, 2007). Utilizing consensus network analysis, we identified modules shared across independent nerve injury data sets and calculated the first principal component of gene expression in each module (module eigengene). Next, we correlated the module eigengenes with time after nerve injury to select modules; from the identified modules based on intramodular connectivity we selected the hub genes for experimental validation. Candidate genes were, *Smagp* (small trans-membrane and glycosylated protein), *Gfpt1* (glutamine fructose-6-phosphate transaminase 1), *Tslp* (thymic stromal lymphopoietin), *Nudt6* (nucleoside diphosphate linked moiety X-type motif 6), *Cdc42se2* (CDC42 small effector 2), *Rfxap* (regulatory factor X-associated protein), *Grem2* (gremlin 2), and LOC688459. The consensus networks after sciatic nerve injury from two different datasets (GSE30691, GSE26350) can be found in the following links: https://coppolalab.ucla.edu/gclabapps/nb/browser?id=Consensus_Tuszynski;ver=vijay
https://coppolalab.ucla.edu/gclabapps/nb/browser?id=Consensus_Fainzilber;ver=vijay

Gene Ontology, Pathway and Pubmed Analyses

Gene ontology and pathway enrichment analysis was performed using the DAVID platform (DAVID, https://david.ncifcrf.gov/ (Huang da et al., 2009)). A list of differentially regulated transcripts for a given modules were utilized for enrichment analyses. All included terms exhibited significant Benjamini corrected P-values for enrichment and generally contained greater than five members per category. We used PubMatrix (Becker et al., 2003) to examine each module's association with neuronal regeneration based on the published literature by testing association with the key-words neuronal regeneration, axonal regeneration, and nerve injury in the PubMed database for every gene.

Knowledge-Based Semi-Supervised Approach

In this approach, we first generated pairwise gene co-expression networks consisting of genes with a correlation coefficient $R > 0.8$ and P-val < 0.01 (t-test). Then we applied a Markov clustering algorithm (MCL) to detect highly correlating co-expression sub-networks. MCL algorithm is a graph-based clustering algorithm based on graph flow simulation (Dongen, 2008). For the clusters we obtained, we assigned the gene profiles to predefined clusters and calculated the significance of the clusters using The Short Time-series Expression Miner (Ernst and Bar-Joseph, 2006). In parallel, we identified significant genes by computing a regression fit for each gene included in the clusters generated from the MCL algorithm. The significance was calculated by computing a P-value (F-Statistic) with a false discovery rate correction. Overlapping genes from the regression and Markov clustering steps were considered significant and were utilized for screening the PubMed database with the key-words - neuronal / axonal-regeneration, and nerve injury. Based on the association of the genes with these key-words, we segregated the genes into associated-genes and non-associated-genes (knowledge- based classification). Next, we created TF-binding-matrices (presences or absences of TFBS for each gene) for associated and non-associated genes by screening for TFBS on their promoter sequence using the PWMs of 130 experimentally validated binding- sites from JASPAR database (Portales-Casamar et al., 2010). We utilized the MEME algorithm for predicting the TFBS occurrence (Bailey and Elkan, 1994). Based on the presence, absence, and number of motif occurrence on both TF-binding-matrices, we separated the TFs into various TF-clusters by k-means clustering. Next, we examined the extent of overlap among the

TF-clusters obtained from associated and non- associated TF-binding-matrices. Similar occurrences of patterns/clusters of TFBS in genes are known to be involved in co-operative transcriptional regulation of functionally related genes. Based on the significant overlap (P-value < 0.05) among the TF-clusters we ranked the genes. Depending upon the above mentioned criteria we selected eight genes to examine their role in neurite outgrowth regulation that are not reported previously. The candidate genes were, *Fxyd5* (FXYD domain containing ion transport regulator 5), *Tacstd2* (tumor-associated calcium signal transducer 2), *Kif22* (kinesin family member 22), RGD1304563, *Cldn4* (claudin 4), *Fam46a* (family with sequence similarity 46, member A), *Pdcl3* (phosducin-like 3), and *Rrad* (Ras-related associated with diabetes).

Over-expression of Novel Candidate RAGs

Sixteen lentiviral ORF expression clones (candidate regeneration associated genes) and control vector (pReceiver-Lv122) were purchased from GeneCopoeia (Rockville, MD). For viral production, psPAX2 and VSVG (both http://www.addgene.org) were used for viral packaging and envelope, respectively. Viruses were prepared by transfecting early-passage 293T cells (ATCC, Manassas, VA) using Fugene 6 (Promega, Madison, WI). Viral media containing 5mg/mL polybrene was centrifuged at 3000 rpm for 5 minutes to clear cell debris, and supernatant was filtered through a 0.45 uM filter. Viral titers of at least 105 particles/mL were verified using Lenti-Go-Stix (Clontech, Mountain View, CA). Viral stocks were used to transduce DRGs for 24 hours. On the next day, an equal amount of fresh medium (1:1) was added to each well. The media were then changed every two days. One week after infection, DRG cultures were trypsinated (0.25%) and replated on to a 24 well glass plate with coverslips. The overexpression achieved through lentiviruses resulted in more than 95% infection efficiency. The cells were fixed with 4% paraformaldehyde 24 hours after replating. Fixed cells were immunostained for anti-beta tubulin (1:800, Sigma, RRID:AB_1844090). Neurite initiation and the longest neurite length of the cells expressing GFP and immunostained for beta tubulin were quantified using NeuroMath and ImageJ software (NeuronJ plugin). Data were obtained from at least three separate experiments. The statistics was done for n = 3, with all cells from one experiment averaged as a single value. Over-expression of candidate RAGs did not cause a significant change in the number of DRG neurons that survived re-plating (for example: control: 65.0 ± 2.3 cells per 10X field; Candidate RAG over-expression: 62.0 ± 3.8 cells per 10X field; p = 0.18 (Student's two-tailed t-test).

Transcription Factor Overexpression

The pLenti CMV mCherry GFP plasmid was produced by modifying pLenti CMV GFP Puro (Addgene). The PGK promoter-PuroR sequence was removed using EcoRI and KpnI restriction sites. EGFP was removed using XbaI and SalI and replaced by a synthesized mCherry-2A-EGFP sequence (Life Technologies) via Gibson Assembly (New England BioLabs). The pLenti CMV mCherry GFP was used as a control. For Atf3 and Jun overexpression, mCherry was replaced by mouse Atf3 or Jun using XbaI and SalI to create pLenti CMV Atf3 GFP and pLenti CMV Jun GFP. Lentivirus was produced at the Boston Children's Hospital Viral Core. Lentivirus (50,000 viral genomic copies/neuron) was added to dissociated mouse DRG cultures at 1 DIV with 5 µg/ml protamine sulfate. Neurons were trypsinized and re-plated at 7 DIV onto PDL + laminin and cultured for an additional 20 hours for neurite outgrowth.

Knock-down of Novel Candidate RAGs

Mission control plasmid containing either shRNA sequences to *Fxyd5*, *Gfpt1*, *Smagp*, *Tacstd2* and *Cdc42* were purchased from Sigma-Aldrich and shRNA control vector, containing a non-specific shRNA, was purchased from Open-Biosystems. GFP was subcloned into the pLK0.1-puro. Plasmid CSCGW2 was cut with Nhe1 and Kpn1 to obtain the eGFP fragment, which was then subcloned into pLK0.1-puro cut with Spe1 and Kpn1, ablating the Spe1/Nhe1 site. Viral particles were produced as previously described (Sena-Esteves et al., 2004). One hour after plating the DRG neurons, 100MOI of $shRNA^{control}$ or $shRNA^{Fxyd5}$, $shRNA^{Gfpt1}$, $shRNA^{Smagp}$, $shRNA^{Tactd2}$, $shRNA^{cdc42}$ were added to the DRG cultures and incubated for 24 hours. On the next day, an equal amount of fresh medium (1:1) was added to each well. The media were then changed every two days. One week after infection, DRG cultures were trypsinated (0.25%) and replated on to a 8 well glass plate with a density of 1,500 cells per field. The cells were fixed with 4% paraformaldehyde 17 hours after replating. Fixed cells were immunostained for anti-beta tubulin (1:800, Sigma, RRID:AB_1844090). Neurite initiation and the longest neurite length of the cells expressing GFP and immunostained for beta tubulin were quantified using NeuroMath. Data were obtained from at least three separate experiments repeated in quadruplicate. Measurements were made blinded to treatment.

Transcription Factor Binding Site Enrichment

Transcription factor binding site (TFBS) enrichment analysis was performed by scanning the canonical promoter region (1000bp upstream of the transcription start site) for the genes (kME > 0.5) present in the regeneration-associated co-expression modules. Next we utilized TFBS position weight matrices (PWMs) from JASPAR (205 non-redundant and experimentally defined motifs) and TRANSFAC (2,208 redundant, manually curated database, extracted from the original scientific literature motifs) databases (Matys et al., 2003; Portales-Casamar et al., 2010) to examine the enrichment for corresponding TFBS within each module. For TFBS enrichment all the modules were scanned with each PWMs using Clover algorithm (Frith et al., 2004). To compute the enrichment analysis we utilized three different background datasets (1000 bp sequences upstream of all rat genes, rat CpG islands and rat chromosome 20 sequence). To identify the phylogenetically conserved binding sites, we examined orthologous promoter sequences in humans and mouse sequences. When a TFBS is over-represented (based on the P-values obtained relative to all the three corresponding background datasets) in any of the two organisms we considered it to be phylogenetically conserved, which increases our confidence in these predictions. We also integrated the existing ChIP data for TFs from either ENCODE (Landt et al., 2012) or other compiled genome-wide ChIP data (Lachmann et al., 2010) to generate the regulatory network (Figure 3A).

Western Blot and qRT-PCR

Whole protein lysates of cultured cells were prepared using 0.5% Nonidet P-40 and 250mM NaCl containing the following phosphatase and protease inhibitors: 50mM NaF (Sigma), 100μM NaVO4 (Sigma), 1mM phenylmethylsulfonyl fluoride (Sigma), 1%proteinase inhibitor cocktail (Sigma P8370), and 1mM dithiothreitol (Sigma). 50-80ug of protein was then added to loading buffer containing 50mM dithiothreitol, boiled, and loaded onto SDS-polyacrylamide gel, and proteins were separated using electrophoresis. Gels were transferred onto PVDF membranes using wet-transfer in 20% methanol. Membranes were blocked in TBST + 5% milk for 30 minutes and were probed with primary antibody diluted in blocking buffer at 4ºC overnight. These were then probed with secondary antibody diluted in blocking buffer for one hour at room temperature. Detection was performed using Supersignal West Pico chemiluminescent substrate (Pierce, Rockford, IL). qRT-PCR was performed using an Applied Biosystems 7900 machine according to the manufacturer's instructions. Briefly, RNA was harvested from independent samples overexpressing or knockdown or drug treated cells and cDNA was produced using Superscript III Reverse Transcriptase (Invitrogen) with random hexamers (Invitrogen). SYBR-green was used to quantify amplification of cDNA. Primers we designed using Primer-BLAST (Ye et al., 2012) and was verified to amplify one product by verifying one peak present on the dissociation curves, and standard curves were performed to show that this assay is sensitive to changes in each gene. Three or more biological replicates were used for each condition, and 3 technical replicates were performed for each sample.

Protein-Protein Interaction (PPI) Network Analyses

We constructed an experimentally validated protein–protein interaction (PPI) network using all the regeneration-associated co-expression gene network modules (two up-regulated modules after nerve injury (magenta [394 genes] and pink [74 genes]) and three down-regulated modules (purple [194 genes], darkred [52 genes], and greenyellow [53 genes]) after injury). We created all possible combinations of gene pairs present in these co-expression networks and identified all experimentally verified interaction data (in humans or mouse or rat dataset) for their corresponding proteins in the STRING database (integration of the following databases: BIND, DIP, GRID, HPRD, IntAct, MINT, and PID) (Franceschini et al., 2013), constructing the protein network by force-directed layout using edge betweenness (Figure 4A). The size of each node in the PPI network is determined by its corresponding protein's literature association with neuronal regeneration. For that we determined the association with the following key-words: neuronal-regeneration, axonal-regeneration, and nerve injury in the PubMed database for every protein using R (http://cran.r-project.org/).

In Silico Small Molecule Screening

The Connectivity Map (cmap) database was used for screening and the database details have been described previously (Lamb et al., 2006). In this method, the similarity between the query signature (RAG signature) and more than 7,000 expression profiles for 1,309 compounds (reference signatures) in the cmap database were evaluated (Lamb et al., 2006). Enrichment of both the up- and down-regulated nerve injury-induced genes in the profiles of each treatment instance were estimated with a metric based on the Kolmogorov-Smirnov statistic, (a nonparametric, rank-based pattern-matching strategy) as described (Lamb et al., 2006) and combined to produce a "connectivity score." For the query, the probe ID defined by the Affymetrix GeneChip Human Genome U133A array (Affymetrix, Santa Clara, CA, USA) was used. Here, the probe ID of U133A corresponding to the RAG signatures after injury were mapped using DAVID (Huang da et al., 2009), followed by the query in the cmap database. Permutated results, which consist of the arithmetic means of the connectivity scores, the statistical significance of the replicates and the non-null percentage (calculated as "enrichment", "permutation P value" and "percent non-null" at the cmap), were used to evaluate the significance of the scores and to rank the molecules in order to select the top three molecules for experimental validation. This methodology was applied for two query signatures related to nerve injury: (a) the protein-protein interaction network consisting of 280 genes (Figure 4A), and (b) genes from all of the regeneration-associated co-expression modules (Figure 1 and Table S2a). The top enriched small-molecules intersecting in both the signature lists were utilized for experimental validation.

Neurite Outgrowth Assay in Primary Adult DRG Neuron Culture

DRGs were digested in collagenase (5 mg/ml)/dispase (1 mg/ml) (Roche, Indianapolis, IN), dissociated in 0.25% trypsin (Cellgro, Herndon, VA) and mechanically triturated through a polished Pasteur pipette to a single-cell suspension. Cells were purified on 10% BSA in PBS solution (Sigma, St. Louis, MO) to enrich the cultures for neurons (>90%). Then the cells were plated in a tissue culture eight-well chamber slide dish (Nalge Nunc, Naperville, IL) coated with poly-D-lysine and laminin (Sigma) cultured in Neurobasal medium (Invitrogen, Carls- bad, CA) supplemented with B27 supplement, penicillin, streptomycin, 1 mM L-glutamine, 50 ng/ml NGF, 2 ng/ml GDNF, and 10 mM AraC at 37°C. For drug treatment, adult C57BL/6J dissociated DRG neurons were cultured for 24 hours in the presence of 40 and 60uM concentrations of drugs. The cells were fixed with 4% paraformaldehyde. Fixed cells were immunostained for bIII-tubulin (RRID:AB_2313773). Neurite initiation and the longest neurite length of the cells were quantified using NeuroMath or ImageJ software (NeuronJ plugin). Data were obtained from at least three separate experiments repeated in quadruplicate.

Mice Surgery, Drug Administration and Optic Nerve Injury

All experimental procedures were performed in compliance with animal protocols approved by IACUC at Boston Children's Hospital. Optic nerve from 6 weeks C57BL/6 mice were crushed as described previously (Park et al., 2008) just after intravitreal injection of 1uL of Ambroxol (Sigma- 25mg/ml in 5% Tween80-5% Polyethylen glycol 400 in water) or vehicle (5% Tween80-5% PEG 400 in water). A second intravitreal injection of Ambroxol or vehicle was performed 7 days post optic nerve crush. Daily mice received 120uL (25mg/ml) of Ambroxol or vehicle intraperitoneally, i.e from the day after the optic nerve crush to the day prior of termination.

Regenerating axons were traced by intravitreal injection of 1uL of CTB-Alexa-488 (1ug/uL in PBS- Invitrogen) two days before termination.

Tissue Preparation

Animals were given a lethal dose of anesthesia (Ketamine/Xylazin) and perfused intracardially with 4% Paraformaldehyde (PFA) in PBS. After dissection, samples were post fixed overnight at 4°C in 4% PFA. Optic nerves were cryoprotected in 15% Sucrose/PBS for 48 hours at 4°C. Optic nerves were embedded in Tissu Tek and 14um section were made with cryostat. Sections were washed 3 times 5 min in PBS and mounted with Fluoromont-G. After post fixation, whole retinas were dissected out from the eyeball. Retinas were washed 3 times 10min in PBS. Retinas were incubated for 1h at room temperature in blocking solution (3% BSA, 0,5% Triton X-100 in PBS). Tuj1 antibody (Covance, 1/400, RRID:AB_2313773) was diluted in blocking solution and incubated overnight at 4°C. Retinas were then washed 3 times 10min in 0,1% Triton X-100 in PBS. Secondary antibody (anti-mouse Alexa 594- Invitrogen) was diluted in blocking solution and in incubated 2h at room temperature. Retinas were then washed 3 times 10min in 0,1% Triton X-100 in PBS and mounted with Fluoromont-G.

References:

Bailey, T.L., and Elkan, C. (1994). Fitting a mixture model by expectation maximization to discover motifs in biopolymers. Proc Int Conf Intell Syst Mol Biol *2*, 28-36.

Becker, K.G., Hosack, D.A., Dennis, G., Jr., Lempicki, R.A., Bright, T.J., Cheadle, C., and Engel, J. (2003). PubMatrix: a tool for multiplex literature mining. BMC Bioinformatics *4*, 61.

Blesch, A., Lu, P., Tsukada, S., Alto, L.T., Roet, K., Coppola, G., Geschwind, D., and Tuszynski, M.H. (2012). Conditioning lesions before or after spinal cord injury recruit broad genetic mechanisms that sustain axonal regeneration: superiority to camp-mediated effects. Exp Neurol *235*, 162-173.

Costigan, M., Befort, K., Karchewski, L., Griffin, R.S., D'Urso, D., Allchorne, A., Sitarski, J., Mannion, J.W., Pratt, R.E., and Woolf, C.J. (2002). Replicate high-density rat genome oligonucleotide microarrays reveal hundreds of regulated genes in the dorsal root ganglion after peripheral nerve injury. BMC Neurosci *3*, 16.

Costigan, M., Belfer, I., Griffin, R.S., Dai, F., Barrett, L.B., Coppola, G., Wu, T., Kiselycznyk, C., Poddar, M., Lu, Y.*, et al.* (2010). Multiple chronic pain states are associated with a common amino acid-changing allele in KCNS1. Brain *133*, 2519-2527.

Di Giovanni, S., Knoblach, S.M., Brandoli, C., Aden, S.A., Hoffman, E.P., and Faden, A.I. (2003). Gene profiling in spinal cord injury shows role of cell cycle in neuronal death. Ann Neurol *53*, 454-468.

Dongen, S.V. (2008). Graph Clustering Via a Discrete Uncoupling Process. SIAM J Matrix Anal Appl *30*, 121-141.

Ernst, J., and Bar-Joseph, Z. (2006). STEM: a tool for the analysis of short time series gene expression data. BMC Bioinformatics *7*, 191.

Fischer, D., Petkova, V., Thanos, S., and Benowitz, L.I. (2004). Switching mature retinal ganglion cells to a robust growth state in vivo: gene expression and synergy with RhoA inactivation. J Neurosci *24*, 8726-8740.

Franceschini, A., Szklarczyk, D., Frankild, S., Kuhn, M., Simonovic, M., Roth, A., Lin, J., Minguez, P., Bork, P., von Mering, C.*, et al.* (2013). STRING v9.1: protein-protein interaction networks, with increased coverage and integration. Nucleic Acids Res *41*, D808-815.

Frith, M.C., Fu, Y., Yu, L., Chen, J.F., Hansen, U., and Weng, Z. (2004). Detection of functional DNA motifs via statistical over-representation. Nucleic Acids Res *32*, 1372-1381.

Geeven, G., Macgillavry, H.D., Eggers, R., Sassen, M.M., Verhaagen, J., Smit, A.B., de Gunst, M.C., and van Kesteren, R.E. (2011). LLM3D: a log-linear modeling-based method to predict functional gene regulatory interactions from genome-wide expression data. Nucleic Acids Res *39*, 5313-5327.

Huang da, W., Sherman, B.T., and Lempicki, R.A. (2009). Systematic and integrative analysis of large gene lists using DAVID bioinformatics resources. Nat Protoc *4*, 44-57.

Kadoya, K., Tsukada, S., Lu, P., Coppola, G., Geschwind, D., Filbin, M.T., Blesch, A., and Tuszynski, M.H. (2009). Combined intrinsic and extrinsic neuronal mechanisms facilitate bridging axonal regeneration one year after spinal cord injury. Neuron *64*, 165-172.

Lachmann, A., Xu, H., Krishnan, J., Berger, S.I., Mazloom, A.R., and Ma'ayan, A. (2010). ChEA: transcription factor regulation inferred from integrating genome-wide ChIP-X experiments. Bioinformatics *26*, 2438-2444.

Lamb, J., Crawford, E.D., Peck, D., Modell, J.W., Blat, I.C., Wrobel, M.J., Lerner, J., Brunet, J.P., Subramanian, A., Ross, K.N.*, et al.* (2006). The Connectivity Map: using gene-expression signatures to connect small molecules, genes, and disease. Science *313*, 1929-1935.

Landt, S.G., Marinov, G.K., Kundaje, A., Kheradpour, P., Pauli, F., Batzoglou, S., Bernstein, B.E., Bickel, P., Brown, J.B., Cayting, P.*, et al.* (2012). ChIP-seq guidelines and practices of the ENCODE and modENCODE consortia. Genome Res *22*, 1813-1831.

Langfelder, P., and Horvath, S. (2007). Eigengene networks for studying the relationships between co-expression modules. BMC Syst Biol *1*, 54.

Lim, W.K., Wang, K., Lefebvre, C., and Califano, A. (2007). Comparative analysis of microarray normalization procedures: effects on reverse engineering gene networks. Bioinformatics *23*, i282-288.

Ma, C.H., Brenner, G.J., Omura, T., Samad, O.A., Costigan, M., Inquimbert, P., Niederkofler, V., Salie, R., Sun, C.C., Lin, H.Y., *et al.* (2011). The BMP coreceptor RGMb promotes while the endogenous BMP antagonist noggin reduces neurite outgrowth and peripheral nerve regeneration by modulating BMP signaling. J Neurosci *31*, 18391-18400.

Matys, V., Fricke, E., Geffers, R., Gossling, E., Haubrock, M., Hehl, R., Hornischer, K., Karas, D., Kel, A.E., Kel-Margoulis, O.V., *et al.* (2003). TRANSFAC: transcriptional regulation, from patterns to profiles. Nucleic Acids Res *31*, 374-378.

Michaelevski, I., Segal-Ruder, Y., Rozenbaum, M., Medzihradszky, K.F., Shalem, O., Coppola, G., Horn-Saban, S., Ben-Yaakov, K., Dagan, S.Y., Rishal, I., *et al.* (2010). Signaling to transcription networks in the neuronal retrograde injury response. Sci Signal *3*, ra53.

Oldham, M.C., Horvath, S., and Geschwind, D.H. (2006). Conservation and evolution of gene coexpression networks in human and chimpanzee brains. Proc Natl Acad Sci U S A *103*, 17973-17978.

Oldham, M.C., Konopka, G., Iwamoto, K., Langfelder, P., Kato, T., Horvath, S., and Geschwind, D.H. (2008). Functional organization of the transcriptome in human brain. Nat Neurosci *11*, 1271-1282.

Park, K.K., Liu, K., Hu, Y., Smith, P.D., Wang, C., Cai, B., Xu, B., Connolly, L., Kramvis, I., Sahin, M., *et al.* (2008). Promoting axon regeneration in the adult CNS by modulation of the PTEN/mTOR pathway. Science *322*, 963-966.

Portales-Casamar, E., Thongjuea, S., Kwon, A.T., Arenillas, D., Zhao, X., Valen, E., Yusuf, D., Lenhard, B., Wasserman, W.W., and Sandelin, A. (2010). JASPAR 2010: the greatly expanded open-access database of transcription factor binding profiles. Nucleic Acids Res *38*, D105-110.

Ryge, J., Winther, O., Wienecke, J., Sandelin, A., Westerdahl, A.C., Hultborn, H., and Kiehn, O. (2010). Transcriptional regulation of gene expression clusters in motor neurons following spinal cord injury. BMC Genomics *11*, 365.

Sena-Esteves, M., Tebbets, J.C., Steffens, S., Crombleholme, T., and Flake, A.W. (2004). Optimized large-scale production of high titer lentivirus vector pseudotypes. J Virol Methods *122*, 131-139.

Wang, Y., Tang, X., Yu, B., Gu, Y., Yuan, Y., Yao, D., Ding, F., and Gu, X. (2012). Gene network revealed involvements of Birc2, Birc3 and Tnfrsf1a in anti-apoptosis of injured peripheral nerves. PLoS One *7*, e43436.

Ye, J., Coulouris, G., Zaretskaya, I., Cutcutache, I., Rozen, S., and Madden, T.L. (2012). Primer-BLAST: a tool to design target-specific primers for polymerase chain reaction. BMC Bioinformatics *13*, 134.

Zhang, B., and Horvath, S. (2005). A general framework for weighted gene co-expression network analysis. Stat Appl Genet Mol Biol *4*, Article17.